Major research project

Soluble Decoys to Modulate Complement Receptor Interactions

Author:

Lynn Vermeer

Supervisors:

Dr. Balthasar Heesters

Prof. Dr. Suzan Rooijakkers

Submitted in partial fulfilment of the requirements
for the Master of Science degree

in the

Department of Chemical Biology and Drug Development

Molecular and Cellular Life Sciences

Utrecht University

October 2022

Abstract

The complement system forms an important bridge from innate to adaptive immunity, particularly through complement-mediated antigen presentation in germinal centers (GCs). Here, follicular dendritic cells (FDCs) present antigens within opsonized immune complexes on complement receptors (CRs) to B cells in the context of affinity maturation. Despite the importance of GC reactions for humoral immunity and the detrimental effects of GC dysregulation, the regulatory mechanisms that underlie these processes remain elusive. One prominent hypothesis is that antigen availability, as determined by antigen presentation on FDC-associated CR2, regulates GC activity and, by extent, the humoral immune response.

This research aimed to produce soluble decoy receptors that displace opsonized immune complexes from cell-bound CRs and thereby limit antigen availability, for the purpose of immune modulation and to acquire fundamental knowledge on GC regulation. Three decoy receptors were produced, of which one (termed sCR2.3d) exhibited strong binding to the opsonins C3b, C3d and C4b and was capable of displacing immune complexes from cell-associated CR2. Further research on the immune modulating potential of this decoy and its application to treat (auto-)immune disorders is warranted. Moreover, this research provided new insights into the binding properties of CR1 and CR2, suggesting that CR2 has a high affinity for C3b and C4b in addition to C3d, and that high-affinity binding of CR1 to C3b and C4b requires more binding domains than previously described.

Layman's summary

The immune system is crucial for the body's protection against infection and disease, but in some cases it targets safe compounds or parts of the own body (auto-immunity) that it should not attack. To prevent this, immune cells are trained to recognize and target dangerous compounds, for example during the production of strong antibodies. In this process, developing immune cells are repeatedly presented with so-called *antigens*, which are recognition fragments present on the surface of pathogens or dangerous compounds. Importantly, these antigens are first tagged by the immune system using molecular flags called *opsonins*, and these opsonins allow the antigens to be presented to developing immune cells on so-called *complement receptors*. While we know that this complement receptor-dependent presentation is necessary to make strong antibodies against those specific antigens, we do not yet understand how this process is regulated. More specifically, we do not

know what the effect is of presenting more or less of the same antigen (termed the *antigen availability*).

In this study, we investigated this by creating *decoy receptors* that can "steal" antigens from complement receptors. Three different decoy receptors were made and they were tested to check if they can bind opsonins and if they can steal opsonized antigens from cells. One decoy receptor (called sCR2.3d) was able to strongly bind all the tested opsonins, and it could steal opsonized antigens from cells with complement receptor type 2.

This research is important because it provided new insights into how these complement receptors work and how we can potentially influence their function by decreasing antigen availability. This could eventually be used to treat certain auto-immune or hypersensitivity disorders, since these disorders involve the presentation of "innocent" antigens. By stealing these antigens from complement receptors using our decoy receptors, we could prevent the body from producing strong antibodies and thus prevent the immune system from attacking the own body or a safe compound. More research is needed on the function and safety of these decoys before they could be used in a clinical setting, but they can already be used to study how antigen availability influences antibody production.

Table of Contents

Introduction

The immune system has evolved over millions of years to yield the complex network of biological processes that protect us from disease and infection today. The adaptive immune system with its roughly 500 million years of age is characterized by its pathogen-driven plasticity (Cooper & Alder, 2006; Flajnik & Kasahara, 2009). Innate immunity, however, has been traced back to nearly a billion years ago and many of its components are highly evolutionarily conserved (Wilson & Hunt, 2002; Buchmann, 2014).

A prime example of this evolutionary conservation pertains to the complement system. This collection of innate serum proteins - termed C1 till C9 - has proven essential to protective immunity, as illustrated by the wide range of pathophysiological consequences associated with complement deficiencies (Wen, Atkinson, & Giclas, 2004; Schröder-Braunstein & Kirschfink, 2019) and the elaborate complement evasion strategies employed by pathogens (Rooijakkers & van Strijp, 2007; Lambris, Ricklin, & Geisbrecht, 2008; Garcia *et al.*, 2016). Complement proteins are produced in the liver and circulate in their inactive form until they are proteolytically activated via one of the three complement activation pathways (Merle *et al.*, 2015a). Once activated, the complement system has a variety of effector functions, most notably the induction of inflammation, the promotion of pathogen phagocytosis and the assembly of membrane attack complexes to lyse invading cells (Merle et al., 2015b).

Besides its powerful role in innate immunity, the complement system provides a crucial bridge to adaptive immunity, particularly through the complement opsonization pathway (Bennett, Rooijakkers, & Gorham, 2017). This branch of the complement system relies on the deposition of protein fragments known as *opsonins* on the pathogen surface via a thioester bond and it occurs following alternative, lectin and classical complement activation. The classical opsonization pathway is triggered by the binding of low-affinity antibodies to antigens, as the binding of natural IgM or multiple adjacent IgG antibodies enables the association of the C1q component of the C1 complex to the antibody Fc domains. This binding induces conformational changes in the C1 complex - which consists of C1q, C1r and C1s - that expose the catalytic domain of C1r and allow it to cleave C1s into its active serine protease state. This in turn provokes the cleavage of C4 into C4a and the opsonin C4b, as well as the cleavage of C2 into C2a and C2b. On the pathogen surface, C4b can associate with C2b to form the classical C3 convertase (also known as C4bC2b, formerly C4b2a). This complex catalyzes the cleavage of C3 into C3a and the opsonization fragment C3b. Notably,

a single C3 convertase can cleave over 1000 C3 proteins per second, which enables significant amplification of the complement cascade. On the pathogen surface, C3b cleavage can continue towards iC3b and eventually the more stable opsonin C3d. (Merle *et al.*, 2015a)**(Figure 1)**

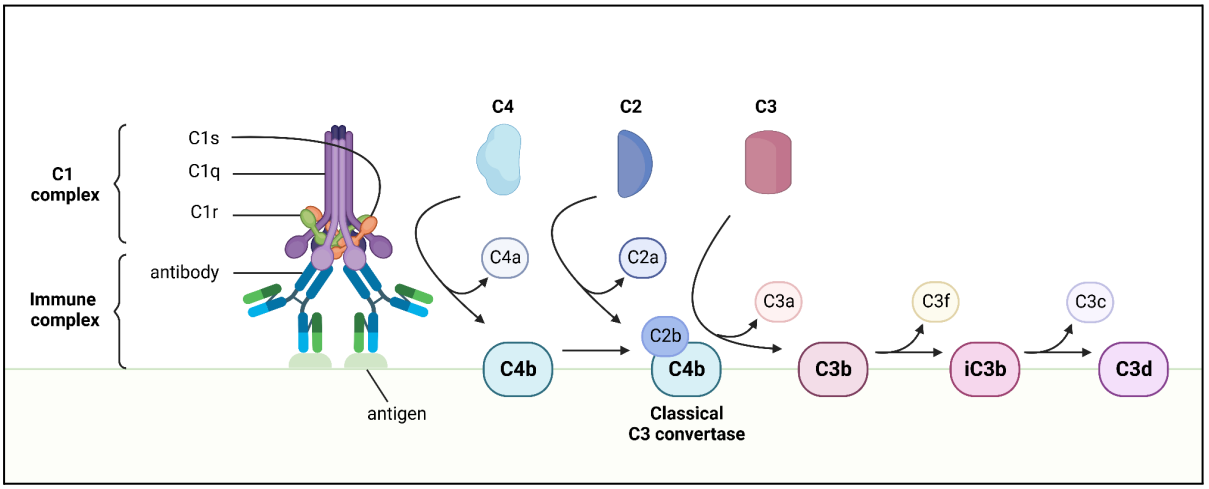

Figure 1. Complement opsonization overview. Immune complexes form when antigens are bound by antibodies. Immune complexes associate with the C1 complex, which initiates classical complement activation. This ultimately leads to the assembly of C4 and C3 convertases and thereby the cleavage of C4 into C4a and C4b, and C3 into C3a and C3b. The C4b and C3b fragments are opsonins that attach to the antigen surface. Further cleavage can remove C3f from C3b and result in the opsonin iC3b, which in turn can be further cleaved into the opsonin C3d by the removal of C3c.

Opsonins serve as recognition fragments for immune cells and are bound by complement receptors (CRs), particularly CR1-4. These receptors are expressed by both innate and adaptive cells, including macrophages, (follicular) dendritic cells and lymphocytes. They often exhibit cross-binding for different opsonins, though with varying affinities. Some complement receptors have ligands other than opsonins, such as CR2 which binds Epstein-Barr virus. Moreover, some receptors possess catalytic domains, such as CR1 that is involved in decay acceleration and complement cascade regulation. An overview of complement receptors, their ligands, catalytic function and associated cell types is provided in **Table 1**.

Table 1. Main complement receptors, ligands and function. FDC = follicular dendritic cell, PMN = polymorphonuclear leukocyte.

Complement receptor	Cluster of differentiation	Expressed by	Main ligands	Other functions

CR1	CD35	B lymphocytes, FDCs, Erythrocytes, Macrophages, Monocytes, PMNs	C3b C4b iC3b	Cofactor and decay acceleration
CR2	CD21	B lymphocytes, FDCs	C3d iC3b Epstein-Barr virus	B cell coactivator
CR3	CD11b + CD18	FDCs, Macrophages Monocytes, PMNs	iC3b	Leukocyte adherence
CR4	CD11c + CD18	Dendritic cells, Macrophages, Monocytes, PMNs	iC3b	Leukocyte adherence

Complement receptors serve as an important link between innate and adaptive immunity, particularly the humoral branch of adaptive immunity that revolves around the production of high-affinity antibodies (Toapanta & Ross, 2006; Roozendaal & Carroll, 2007). This intricate process relies on germinal center reactions that involve fine-tuned collaboration between antigen-specific B cells, T follicular helper cells and follicular dendritic cells (FDCs)(Victora & Nussenzweig, 2012).

In short, germinal centers (GCs) are microanatomical structures that emerge within B cell follicles of secondary lymphoid organs upon antigen acquisition by resting B cells (Cyster, 2010). GCs can be divided into two functionally distinct compartments, namely the light zone and the dark zone (named after their relative appearance in histological stains). In the process of affinity maturation, B cells undergo cycles of somatic hypermutation (SHM) and proliferation in the dark zone followed by antigen-driven selection in the light zone (Mesin, Ersching, & Victora, 2016).

More specifically, the dark zone consists of highly proliferative B cells known as *centroblasts* that express high quantities of activation-induced deaminase (AID) and the error-prone DNA polymerase eta (Polη)(Allen *et al.*, 2007b; McHeyzer-Williams *et al.*, 2015; Victora *et al.*, 2010, 2012). The erroneous Polη-mediated repair of AID-induced lesions enables B cell receptor (BCR) diversification through hypermutation of the BCR variable region, responsible for antigen binding (Maul & Gearhart, 2010). Following SHM and proliferation, these cells migrate to the light zone where they are commonly referred to as *centrocytes* and compete for survival signals associated with high-affinity antigen binding (Victora & Nussenzweig, 2012; Mesin, Ersching, & Victora, 2016).

Antigen presentation in the light zone depends on FDCs that acquire and retain intact antigens within opsonized immune complexes on their complement receptors, particularly CR2 (Heesters, Myers & Carroll, 2014). SHM-modified BCRs are selected for antigen affinity through competitive binding where only the centrocytes with relatively high-affinity binding receive survival signals (Victora & Nussenzweig, 2012). While the exact mechanisms that underlie this positive selection are debated, it is generally accepted that B cell survival is promoted by both BCR signalling and T cell help (Mesin, Ersching, & Victora, 2016). Recent literature highlights the importance of T follicular helper (Tfh) cells in B cell survival through cognate interaction in a feed-forward manner coined *entanglement* (Liu *et al.*, 2014) and the provision of pro-survival cytokines such as B lymphocyte stimulator (BLyS, also known as B cell activating factor [BAFF]) (Goenka *et al.*, 2013).

Importantly, the degree of affinity maturation observed *in vivo* cannot be explained by a single round of hypermutation and selection, but instead relies on iterative cycles of SHM and antigen-driven selection (Meyer-Hermann *et al.*, 2012; Gitlin, Shulman, & Nussenzweig, 2014). Positively selected B cells cyclically re-enter the GC dark zone and the stringency of affinity-based selection in the light zone increases per round, thereby driving directional selection pressure towards BCRs with the highest antigen affinity (Victora *et al.*, 2010; Mesin, Ersching, & Victora, 2016). However, the exact cause of this increased stringency is poorly understood and comprises one of the many enigmas on GC regulation.

A prevalent theory is that decreasing antigen availability on FDCs drives increased selection pressure for B cells per round of affinity maturation (Zhang *et al.*, 2013). This decrease in antigen availability could be attributed to several phenomena, all discovered within the past decade. First is the finding that FDCs cyclically present and internalize antigens, which alters the amount of antigen available for B cell binding at any given time (Heesters *et al.*, 2013, 2014, 2016). Second is the finding that B cells are capable of influencing GC selection via antibody-mediated feedback, where soluble antibodies produced by plasma cells resulting from previous rounds of selection or other GCs “mask” the antigen presented on FDCs (Zhang *et al.*, 2013). This has been shown to limit antigen availability and led to the production of higher-affinity antibodies following later rounds of selection.

Knowledge gaps and current research

Despite these and other recent findings on GC biology, most regulatory mechanisms that underlie GC reactions remain elusive. Relevant knowledge gaps in the field include pathways for antigen uptake and handover (particularly the molecular basis of antigen

transfer from naive B cells to FDCs), the regulation of FDC antigen cycling and subsequent antigen availability or (long-term) retention, the influence of antigen availability on the antibody response, and the regulation of GC lifespan and termination.

The importance of narrowing these knowledge gaps is illustrated by the role of GCs in health and disease. Proper GC function is crucial for adaptive immunity, both in terms of rapid antibody responses and long-term memory. Moreover, GC dysregulation has been associated with autoimmunity, hypersensitivity and cancer (Mesin, Ersching, & Victora, 2016). In particular, prolonged or chronic GCs increase the risk of insufficient negative selection of self-reactive clones leading to autoimmune activity (Vinuesa, Sanz, & Cook, 2009), and excessive AID-induced mutations have been shown to induce B cell lymphomas (Robbiani *et al.*, 2015). It should also be noted that GC-targeted immune modulation could reduce the humoral immune response for pre-existing autoimmune or hypersensitivity disorders, a potential clinical avenue that warrants further research.

In this light, FDCs and their CRs are appealing targets for immune modulation. It is hypothesized that antigen availability, as determined by CR-mediated presentation on FDCs, influences GC longevity and the humoral immune response. Another hypothesis is that soluble decoy receptors can competitively inhibit CRs and thereby limit antigen availability, which can be beneficial to subdue the antibody response or trigger GC shutdown.

That said, this research aims to modulate the humoral immune response by competitively inhibiting CRs on FDCs. It explores the inhibitive capacity of soluble decoy receptors that bind opsonins and can thereby displace opsonized antigens from cell-bound CRs. The specific objectives of this project include (1) the optimization of an *in vitro* IC-CR binding assay, (2) the production of soluble decoy receptors for CR1 and CR2, and (3) the characterization of the blocking capacity of these decoy receptors.

This research is relevant to generate fundamental knowledge on GC reactions and the underlying mechanisms by which they are regulated. It will narrow the knowledge gap on the role that antigen availability - as determined by presentation on FDC-associated CRs - plays in GC regulation and the resulting humoral immune response. Additionally, it will provide tools such as binding assays and decoy receptors with scientific value for the study of CR-dependent processes in a broader context. Finally, it will pave the way for translational applications and contribute to the development of novel immune modulation strategies that target the complement system and GC reactions.

Methods

Cell culture

Raji lymphoma cells (American Type Culture Collection® CCL-86™) and U937 cells (American Type Culture Collection® CRL-1593.2™) were cultured in Iscove's Modified Dulbecco's Medium (IMDM) with high glucose, L-Glutamine and 25 mM HEPES (Gibco™ #12440053) supplemented with 10% (vol/vol) fetal calf serum (FCS) and 0.25% (vol/vol) Pen-Strep. Cells were passaged every 4-5 days at an average split ratio of 1:10 by pelleting and resuspension in fresh medium. HEK293T cells (American Type Culture Collection® CRL-1573™) were cultured in Dulbecco's Modified Eagle Medium (DMEM) with high glucose and L-glutamine (Gibco™ #41965039) supplemented with 10% (vol/vol) FCS and 0.25% (vol/vol) Pen-Strep. Cells were trypsinized and passaged every 3-4 days at an average split ratio of 1:12. All cells were maintained at 37°C and 5% CO_2 in an incubator with humidified atmosphere.

HEK293T and U937 cell lines transduced for the stable expression of human complement receptors (HEK-CR1, -CR2, -CR3 and -CR4 and U937-CR1, -CR2, -CR3 and -CR4) were kindly provided by Prof. Dr. Suzan Rooijakkers (UMC Utrecht) and cultured identically to their wildtype equivalents.

Decoy receptor design and cloning

Soluble decoy receptors were constructed by attaching the binding domain of human CRs to a human IgG1 Fc tail via a valine-serine linker, as first described by Hebell, Ahearn and Fearon (1991). Strep-Tag® II was attached to the Fc domain for detection and purification. This decoy design is illustrated in **Figure 2**.

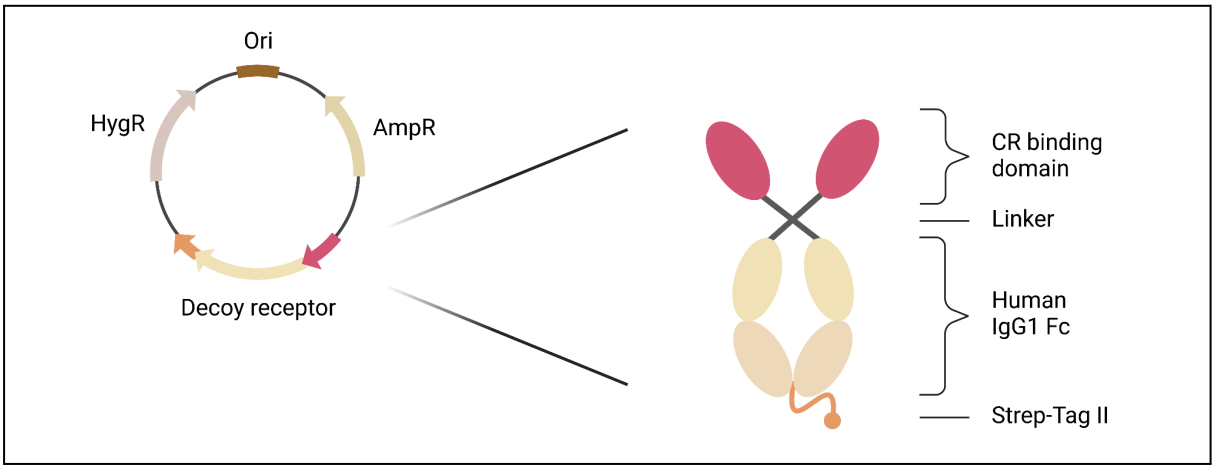

Figure 2. Decoy receptor design. Human CR binding domains were attached to human IgG1 Fc via a valine-serine linker. Strep-Tag® II was attached to this construct for detection and purification. The construct was expressed in the pcDNA™ 5/TO Mammalian Expression Vector (ThermoFisher #103320) encoding ampicillin resistance (AmpR) and hygromycin resistance (HygR) for selection. *Ori = origin of replication.*

Three distinct decoy receptors were constructed, varying only in their binding domain. Binding domain localization (as indicated by short consensus repeats termed *sushi repeats*) and expected ligands were based on literature. One decoy contained the C3d binding domain of CR2 (constituted by CR2 sushi repeats 1-2) and was named soluble CR2.3d / sCR2.3d. Two decoys contained binding domains of human CR1, namely the expected C3b binding domain (sushi repeats 8-9) and the expected C4b binding domain (sushi repeats 1-2). These decoys were named sCR1.3b and sCR1.4b, respectively.

The inserts encoding the CR binding domains were optimized for protein expression based on the OptimumGene™ algorithm and delivered in the pUC57 carrier plasmid (GenScript® #SD1176). Ordered sequences and corresponding binding domains are shown in **Table 2**.

Table 2. Decoy receptor constructs. Legend: *Extra nucleotides for cloning*; binding domain; **LINKER**.

Construct name	CR	Sushi repeats	Binding domain	Optimized sequence (5' → 3')
sCR2.3d	CR2	1-2	C3d	*gtacattct*atctcttgtggctcccccccccctattctgaacgggcggatttcttattactcaa ctcctatcgctgtgggcactgtcattcggtactcttgcagcggcaccttccggctgatcgg cgagaagagcctgctgtgcatcaccaaggacaaggtggatggcacatgggacaagcc cgcccctaagtgcgagtactttaacaagtatagctcctgtccagagcccatcgtgcctgg cggctacaagatccggggctccacaccctatagacacggcgattctgtgaccttcgcctg caagacaaatttttccatgaacggcaataagtccgtctggtgtcaggctaacaatatgtgg ggacctactcggctgccaacctgcgtctcc**GTTTCT***gc*
sCR1.3b	CR1	8-9	C3b	*gtacattct*ggccactgccaggctcctgaccacttcctgttcgccaaactgaaaacccag accaacgcttccgacttcccaatcgggacttctctgaagtacgagtgccggccagagtac tatggcagacccttcagcatcacctgtctggacaacctggtgtggagctcccctaaggac gtgtgcaagcggaagtcctgtaagaccccacctgacccagtgaacggaatggtgcacg tgatcacagatatccaagtgggctccaggatcaattattcttgcaccacaggccaccgcct gatcggacactctagcgccgagtgtattctgtcaggcaatgcagcacactggagcacta aaccaccaatctgtcagcgg**GTCAGC***gc*

sCR1.4b	CR1	1-2	C4b	*gtacattct*cagtgtaacgccccagagtggctgcctttcgcacgaccaaccaacctgaca gatgagtttgagtttcctatcgggacatacctgaactacgagtgcaggccaggatatagc ggccgcccccttctccatcatctgtctgaagaactccgtgtggaccggcgcaaaggacag atgccggcggaagtcttgtaggaacccccctgatcccgtgaatggcatggtgcacgtga tcaagggcatccagtttggctctcagatcaagtacagctgcaccaagggctatcggctga tcggcagctcctctgccacatgtatcatcagcggcgatacagtcatctgggacaacgaaa caccaatctgcgataga**GTGAGC***gc*

The ordered inserts were amplified out of their carrier plasmid for Gibson Assembly® into the pcDNA™ 5/TO Mammalian Expression Vector (ThermoFisher #103320) adapted by Rodrigues *et al*. (2020) to encode the human IgG1 Fc attached to Strep-Tag® II.

Plasmids were transformed into JM109 Competent Cells (Agilent #200235) following the manufacturer's instructions. Plasmid DNA was purified using the Qiagen™ QIAprep Spin MiniPrep Kit (#27104) and subsequently amplified and sterilized using the Qiagen™ Plasmid Maxi Kit (#12162) according to the manufacturer's protocol. DNA yield and purity were determined using a NanoDrop™ device and gel electrophoresis, and cloning was verified using a restriction check and sequencing.

Protein expression

Two days prior to transfection, HEK293T cells were seeded in their usual medium in 150mm Corning® treated culture dishes (#CLS430599) at 15-20% confluency to enable 40-50% confluency on the day of transfection. Transfection was performed by incubating DNA with polyethylenimine (PEI) at a 1:8 (mass/vol) ratio in DMEM without FCS for 30 minutes at room temperature. This mixture was added to the cells drop-wise to provide 40 µg of Maxiprep-derived DNA per 150mm dish. After 5-6 hours, the medium was replaced with SFM II medium (Gibco #11686029) supplemented with Primatone (3 g/L), carbonate (3.6 g/L), glucose (2 g/L), valproic acid (0.4 g/L), 0.1% Glutamax and 0.15% DMSO.

Proteins were harvested 4 days post-transfection. Cell medium containing the soluble, secreted proteins was centrifuged and the supernatant was incubated with Strep-Tactin Sepharose beads (IBA #21201002) overnight to bind the proteins of interest. The beads were then washed and eluted to obtain purified protein. Expression and purity were verified based on Western Blot using the StrepMAB-Classic HRP conjugate (IBA-Lifesciences #2-1509-001), Coomassie Blue staining and NanoDrop™ measurement.

Immune complex generation

B-Phycoerythrin immune complexes (PE-ICs) were generated by incubating B-Phycoerythrin (SureLight™ Cayman Cat: 16632)(1 mg/mL) with rabbit IgG anti-B-Phycoerythrin (Rockland Cat: 100-4199)(10 mg/mL) at a 1:8 volume ratio in gelatin HEPES buffer with Ca^{2+} and Mg^{2+} (GHB++) with 10% (vol/vol) serum for 30 minutes at 37℃. As negative controls, samples with heat-inactivated (HI) serum, no serum, or no B-Phycoerythrin (PE) and anti-B-Phycoerythrin (anti-PE) were included. HI serum was prepared by incubating fresh serum for 30 minutes at 56℃.

ELISA

Nunc Maxisorp™ flat-bottom 96-well plates (ThermoFisher #44-2402-21) were coated overnight at 4℃ with 100 uL of 1 ng/uL purified C3b, C3d or C4b (kindly provided by Dr. Søren Egedal Degn, Aarhus University). The plates were washed with phosphate-buffered saline (PBS)(ThermoFisher #10010023) and blocked with PBS + 1% bovine serum albumin (BSA)(Sigma-Aldrich #9048-46-8) for one hour at RT. The plates were then incubated for 2 hours at RT with a 2-fold serial dilution of decoy receptors in blocking buffer with a maximum concentration of 40 ng/µL in 100 µL (in triplo, including no-coat and no-decoy controls). Subsequently, the plates were washed with PBS and incubated with 1:2000 StrepMAB-Classic HRP conjugate antibody (IBA-Lifesciences #2-1509-001) for one hour at RT. The wells were then washed and incubated with 100 µL of TMB Substrate Solution (ThermoFisher #N301) for 5 minutes at RT, followed by deactivation with 100 µL of 2M H_2SO_4 and detection of decoy binding based on absorbance at 450 nm.

Binding and blocking assay

An IC-CR binding assay was optimized for PE-αPE ratio and IC-cell ratio using Raji cells that naturally express CR2. To this end, Raji cells were incubated for 30 minutes at 37℃ with PE-ICs, washed, and subsequently analyzed using flow cytometry to detect CR2-bound PE-ICs based on PE fluorescence. Data were collected using the BD FACSCanto II machine and analyzed using CytoFlow software.

This binding assay was adapted into an optimized blocking assay on U937 cells. The cells (U937-WT, -CR1, -CR2 and -CR3) were seeded in a round-bottom 96-well FACS plate (Corning™ #38018) at 0.1 x 10^4 cells/well. They were incubated for 30 minutes at 4℃ with PE-ICs and washed with PBS, followed by a 30 minute incubation at 4℃ with 1 µg/well of

decoy receptor. Cells were then washed and resuspended in FACS buffer (1xPBS, 5% (v/v) FBS, 2 mM EDTA, 2 mM NaN_3) for flow cytometry analysis to detect cell-bound PE-ICs. Data were collected using the BD FACSCanto II machine and analyzed using CytoFlow software. Controls with HI-serum, no serum and no ICs were included and all samples were run in triplo. Additional controls included a no decoy condition and a Siglec construct derived from Rodrigues et al. (2020) that shares the decoy framework but contains a Siglec instead of the CR binding domain. A graphical overview of this blocking assay is provided in **Figure 3**.

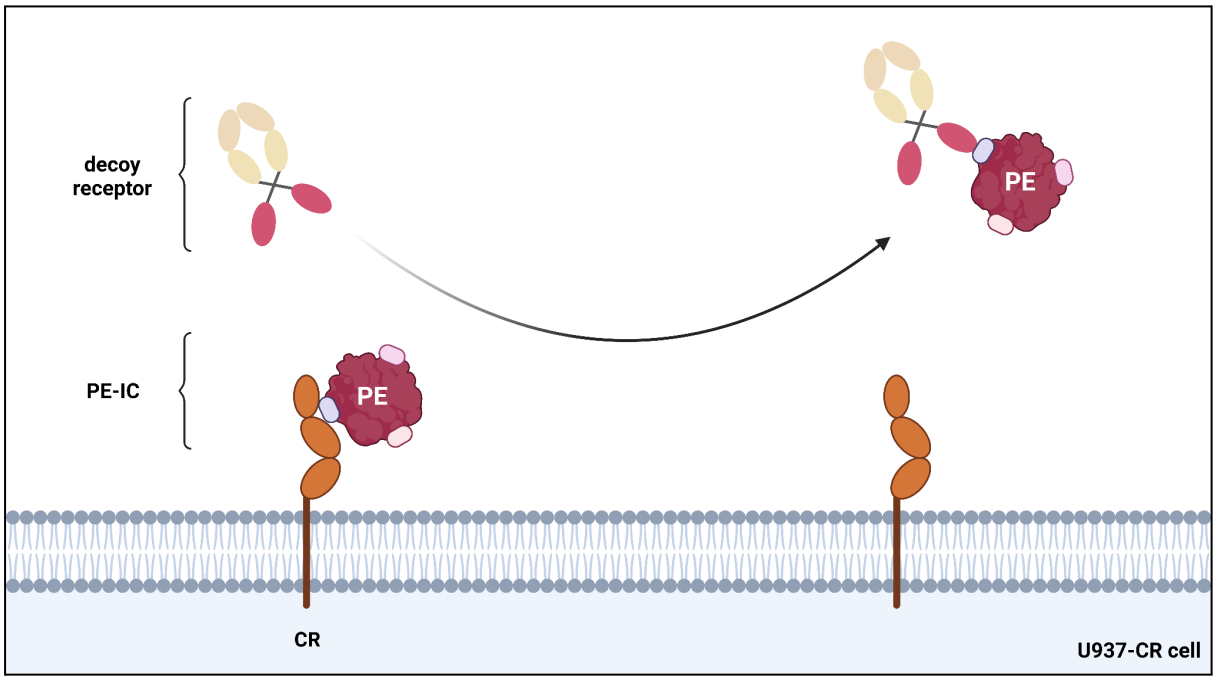

Figure 3. Blocking assay overview. U937 cells expressing cell-surface human CRs (1-3) or wildtype are incubated with PE-ICs to allow complement-mediated CR binding. Decoy receptors containing the binding domains of human CRs are then added to competitively inhibit cell-bound CRs by displacing PE-ICs from the CRs. IC binding and decoy blocking are analysed based on PE signal in flow cytometry.

Results

Decoy receptor expression

Cloning of the decoy receptor inserts into the pcDNA™ 5/TO vector was confirmed using a restriction check with AgeI and SalI digestion (**Figure 4A**). All tested colonies and corresponding samples yielded a band at the expected insert size of ~400 bp and a band at the expected backbone size of ~6000 bp, except for sample sCR1.4b-2 where the latter was shifted downwards. This sample was discarded and only samples sCR1.3b-1, sCR2.3d-1 and sCR1.4b-1 were sequenced (**Figure 4B**). Alignment of the sequences obtained with the expected cloning products showed complete overlap and these samples were subsequently used for protein expression.

Western Blotting of the protein expression cell supernatant resulted in clear bands for all constructs (**Figure 4C**). The sCR1.3b construct yielded the strongest band, followed by the sCR2.3d construct. Total cell lysates from the expression plates also yielded clear bands. After purification of the decoy receptors, Coomassie Blue staining showed clear and specific bands at the expected molecular weight of ~100 kD for all constructs and elutions (**Figure 4D**).

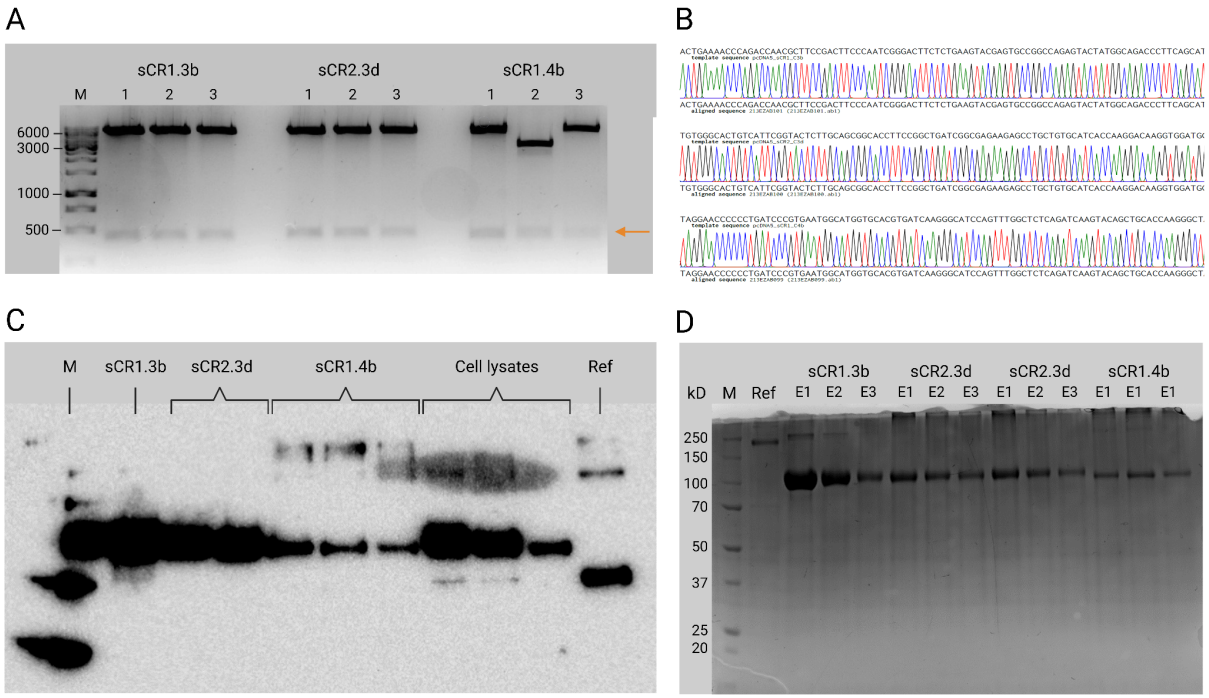

Figure 4. Cloning and protein expression. A) Restriction check with AgeI and SalI digestion. Cut inserts visible around 400 bp (orange arrow) in all samples, cut backbones visible around 6000 bp in all samples except sCR1.4b-2 where the backbone band was shifted downwards. *M = GeneRuler 1kb DNA marker*. B) Sequencing alignments of samples sCR1.3b-1, sCR2.3d-1 and sCR1.4b-1. Partial sequences shown, full sequences available

upon request. sCR1.3b (up), sCR2.3d (middle), sCR1.4b (down). C) Western Blot. Clear bands visible for all samples. Detection using StrepMAB-Classic HRP 1:3000 on 10µL/lane of supernatant from protein expression plates (or total cell lysates). *M = Bio-Rad Precision Plus Protein Marker. Ref = 400 ng reference protein (Siglec Fc construct).* D) Coomassie Blue stain. Clear and specific bands visible around ~100 kD for all samples. Loaded with 10µL/lane of purified protein. *M = Bio-Rad Precision Plus Unstained Protein standards, Ref = 200 ng reference protein (Siglec Fc construct), E = elution round.*

ELISA

The binding capacity of the decoy receptors to the opsonins C3d, C3b and C4b was demonstrated using an ELISA binding assay (**Figure 5**). While sCR2.3d yielded (near-)sigmoidal binding curves for all three opsonins, sCR1.3b and sCR1.4b showed no binding to C3d and only minimal binding to C3b and C4b. The negative control (Siglec Fc construct) showed no binding. These findings are summarized in **Table 3**.

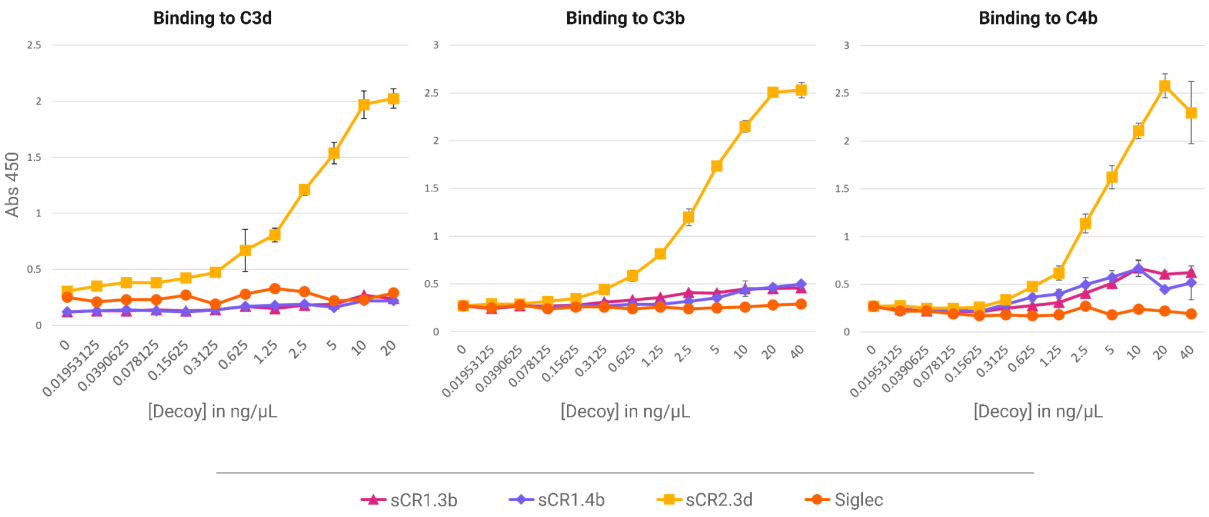

Figure 5. ELISA binding assay. sCR2.3d showed strong binding to all opsonins, whereas sCR1.3b and sCR1.4b only showed minimal binding to C3b and C4b. Data represent the mean of three replicates +/- 1 SD. Plates were coated with 100 µL of 1 ng/µL purified opsonin (C3b, C3d or C4b). *Siglec = Siglec Fc construct, negative control.*

Table 3. Binding capacity of decoy receptors to purified opsonins.

	sCR2.3d	sCR1.3b	sCR1.4b
C4b	++	+	+
C3b	++	+	+
C3d	++	-	-

++ strong binding, + weak binding, - no binding.

Binding assay optimization

PE and anti-PE were both two-fold diluted resulting in a checkerboard 96-well plate with volume ratios ranging from 256:1 to 1:556 (Supplementary Table S1). The incubation of these PE-IC mixes with Raji cells resulted in a range of PE signals (**Figure 6A**). Lymphocyte and single cell gates are shown in Supplementary Figure S1. Comparing the mean geometric PE of all samples revealed that there were local optima for each row at a PE:anti-PE volume ratio of 1:8 (**Figure 6B**) which corresponds to one molecule of PE to 128 molecules of anti-PE. Comparing only the PE:anti-PE 1:8 volume ratio samples illustrated that higher amounts of PE and anti-PE resulted in more PE signal (**Figure 6C**), which enabled the identification of an IC-to-cell ratio for this assay at 1 µL of PE per 100,000 Raji cells to enable the detection of potential blocking effects.

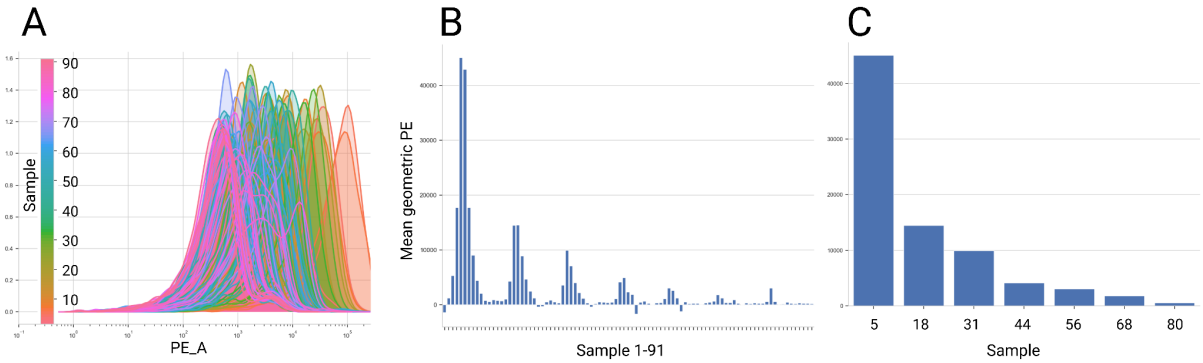

Figure 6. IC-CR binding assay optimization. A) PE_A 1D Kernel Density Estimation, all samples. Sample designations and corresponding PE:anti-PEvolumes shown in Supplementary Table S1. B) Mean geometric PE, all samples. Local optima visible at PE:anti-PE 1:8 volume ratio samples. C) Mean geometric PE, only PE:anti-PE 1:8 volume ratio samples.

Blocking assay

The capacity of the decoy receptors to competitively inhibit ("block") cell-bound CRs was determined using the previously optimized blocking assay. Data were filtered to only include U937 and single cells (Supplementary Figure S2). No serum and HI serum conditions yielded no PE signal on all cell types and U937-WT cells were PE-negative across all conditions (**Figure 7**). On U937-CR1 cells, no decrease in PE signal was observed for any of the decoys compared to the no decoy condition, while the Siglec condition showed a slight increase in PE signal compared to the no decoy condition. On U937-CR2 cells, a significant decrease in PE signal (p=0.0002) was observed for the sCR2.3d decoy compared to the no

decoy condition, while the sCR1.3b decoy yielded a mild decrease and the sCR1.4b and Siglec conditions resulted in an increased PE signal compared to the no decoy condition.

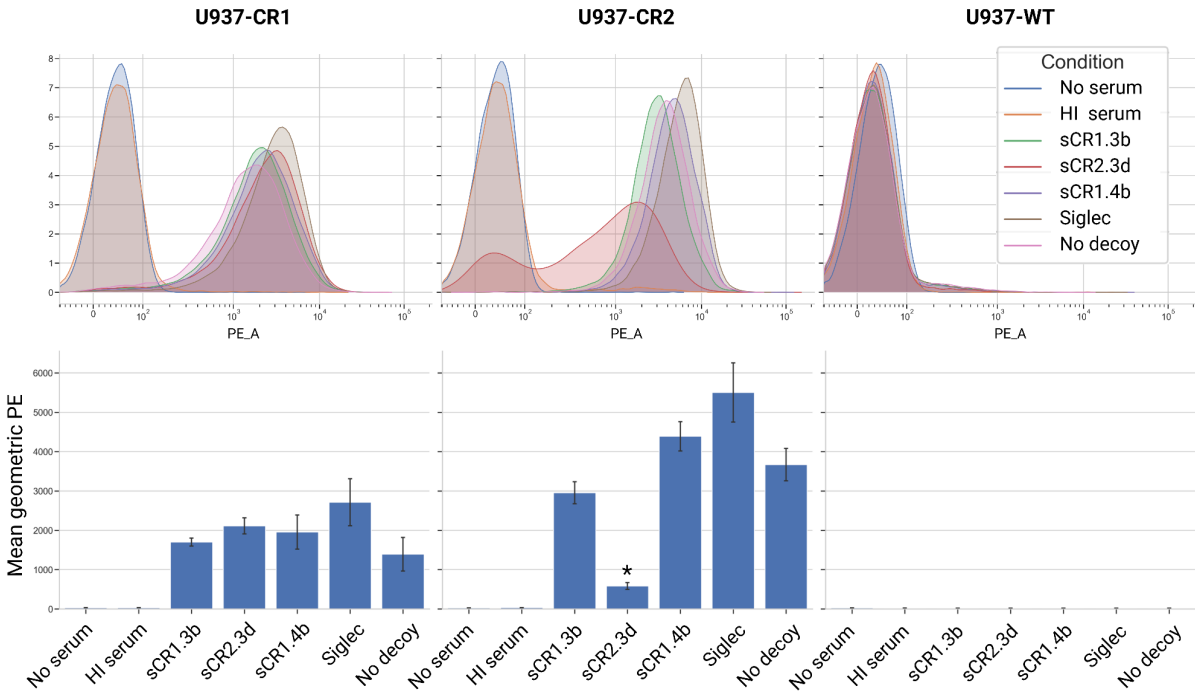

Figure 7. Blocking assay. PE_A signal (up) and mean geometric PE (down) per condition on U937-CR1, U937-CR2 or U937-WT cells. Data filtered for U937 and single cells (Supplementary Figure S2). Data represent the mean of three replicates +/- 1 SD. No serum and HI serum conditions yielded no PE signal on all cell types and U937-WT cells were PE-negative across all conditions. The PE signal in the sCR2.3d condition on U937-CR2 cells was significantly reduced (p=0.0002) compared to the no decoy condition on these cells. Significance was calculated using an unpaired t-test with an α-level of 0.05% and 99% confidence. *Siglec = Siglec Fc construct.*

Discussion

Decoy receptor binding

The ELISAs indicate that the sCR2.3d decoy strongly binds not only C3d but also C3b and C4b. While it has been previously demonstrated that the C3d-binding domain of CR2 (constituted by sushi repeats 1-2) alone is capable of binding C3d without the need of other domains (Lowell *et al.*, 1989; Hebell, Aheurn & Fearon, 1991) and past studies have demonstrated that CR2 can bind iC3b (Kalli, Ahearn & Fearon, 1991), it is remarkable that the C3d-binding domain is sufficient for the strong binding of C3b and C4b. Although the current assays do not facilitate the calculation of binding affinities, the binding curves suggest that the C3b- and C4b-binding capacity of sCR2.3d (and therefore CR2 sushi repeats 1-2) resemble its C3d-binding capacity. This has not been previously described and challenges the view that CR2 only exhibits high-affinity binding of C3d.

The sCR1.3b and sCR1.4b decoys on the other hand show no binding to C3d and only minimal binding to both C3b and C4b in the current assay. This is in line with literature that describes that the designated CR1 C3b- and C4b-binding domains have affinity for both C3b and C4b, while no binding of CR1 to C3d has been observed (Wymann *et al.*, 2021). However, the exact binding domains and affinities of CR1 are highly debated and it is feasible that a decoy containing only two sushi repeats is insufficient to mimic the full binding potential of CR1. This could explain why no strong binding is observed for sCR1.3b and sCR1.4b while the sCR2.3d binds C3b and C4b strongly. In line with this, a proposed binding mechanism of CR1 involves multiple domains throughout the receptor rather than two adjacent sushi repeats, in contrast to CR2 (Liu & Niu, 2009). It should also be noted that the current assay does not account for the potential role of avidity in CR binding.

Altogether, these results suggest that the sCR2.3d decoy can strongly bind C3b-, C3d- and C4b- opsonized immune complexes, while the sCR1.3b and sCR1.4b decoys may only show low-affinity binding to C3b- and C4b-opsonized immune complexes. In addition to the potential application of these decoys for antigen displacement and immune modulation, these findings shed new light on the enigmatic binding domains and properties of CR1 and CR2, which calls for further research. A potential avenue to create higher-affinity CR1 decoys could be to include larger binding domains or different combinations of sushi repeats, though the downside of this would be the increased size and molecular weight of these decoys, potentially limiting their expression and application. Other ways to elaborate this binding

assay would be to experiment with different strategies and densities of opsonin coating and to test a larger set of decoy concentrations to establish binding affinities.

Complement receptor blocking

A significant blocking effect was observed with the sCR2.3d decoy on U937-CR2 cells, which implies that the sCR2.3d decoy is capable of displacing PE-ICs from cell-bound CR2. This is in line with the results of Hebell, Ahearn and Fearon (1991) who expressed a similar CR2 decoy and demonstrated that its administration caused a decreased antibody response in mice. On the U937-CR2 cells, the sCR1.3b condition resulted in a slightly decreased PE signal whereas the sCR1.4b condition led to a slightly increased PE signal compared to the no decoy control. The Siglec condition also showed an increased PE signal compared to the no decoy control. However, these changes were not statistically significant.

On the U937-CR1 cells, none of the decoys led to a decreased PE signal compared to the no decoy control. In fact, the no decoy control showed a lower PE signal than the three decoy conditions and the Siglec control, albeit not significantly. It should be further explored that the no decoy conditions in this experiment did not result in the highest PE signal (together with the Siglec control) as was initially expected. Further optimization of the assay or the IC-to-cell ratio could overcome this, since this effect was not observed in preliminary blocking experiments on Raji cells (Supplementary figure S3).

It is remarkable that the sCR2.3d decoy lead to a decreased PE signal on the U937-CR2 but not the U937-CR1 cells. A potential explanation for this observation is that full-length CR1 has been suggested to employ an IC-binding mechanism where it wraps around the bound IC using additional domains (Liu & Niu, 2009), thereby sterically hindering the access of decoy receptors to the IC-associated opsonins. It should also be noted that although all U937-CR cells were checked for CR expression using specific anti-CR antibodies and flow cytometry (indicating near 100% CR+ cells), it is not known how many CRs are expressed per cell. It is conceivable that one cell line (in this case potentially the U937-CR1 line) expressed more CRs per cell, requiring more decoy receptors to displace the ICs from every receptor and render the cell PE negative.

Altogether, these results demonstrate a promising blocking potential of the sCR2.3d decoy, yet they also indicate that the assay in question needs to be further optimized and that the behaviour of these decoys in biologically relevant assays needs to be further explored before definite conclusions are drawn on their potential therapeutic use. Further optimizations or controls for the blocking assay include checking for CR-mediated IC internalization and

higher decoy-to-IC ratios, as well as blocking assays with a titration of decoy receptor concentrations. Preliminary data showed concentration-dependent blocking of the sCR2.3d decoy on Raji cells (Supplementary Figure S3), yet this was not further explored in the current project due to time restraints.

Optimizations and limitations

The methods and assays described underwent extensive optimization. For the protein expression, a different vector (i.e. AbVec2.0-IGHG1 with His-Tag [AddGene #80795]) was initially used, but the protein yield was very low using both Protein G resin and Nickel purification. As such, the switch to the pcDNA™ 5/TO vector and Strep-Tag purification was made and this yielded sufficient amounts of decoy. Detection of the decoys was also facilitated by this switch, as Strep-Tag detection using the StrepMAB-Classic HRP antibody was more sensitive and specific compared to several anti-human IgG1 antibodies tested.

As for the ELISA binding assay, an alternative approach was tested where the plates were coated with PE-ICs instead of purified opsonins (Supplementary methods). While this did result in concentration-dependent binding curves for the decoys, the negative controls with HI serum resulted in similar curves, indicating that background signal was interfering with the assay (data not shown). A possible explanation is that (partially) degraded inactivated serum components present in the PE-IC mix enabled decoy binding, since conditions including PE and anti-PE but excluding serum did not yield any signal. Since this could not be verified and this approach did not allow for the distinction between C3b-, C3d- and C4b- binding, the binding assay was fully performed using opsonin-coated plates.

This touches upon a major limitation of the PE-IC binding assay on cells, since the current protocol does not provide clarity on the opsonization status of the ICs. More specifically, it is unclear whether these ICs are mostly C3b-, C3d-, or C4b-opsonized and in what ratios these opsonins are present. This question also pertains to the opsonization of ICs in nature, since it remains unclear if different opsonization patterns serve different functions and if so, what causes ICs to be opsonized differently. This could be studied by using specific complement inhibitors in the PE-IC generation protocol and observing whether this affects CR or decoy binding.

The blocking assay described here was initially optimized for PE-to-anti-PE and IC-to-cell ratio on Raji cells that naturally express CR2. To study the blocking of other complement receptors, the assay was first applied on and optimized for HEK-CR cells (Supplementary methods) and later U937-CR cells. The U937 cells allowed for an easier

protocol and less variance between replicates, since these are suspension cells as opposed to the adherent HEK cells that required trypsinization and fixation before flow cytometry.

In addition, several other assays were attempted such as a PE-IC binding assay on tonsil slices to visualize IC binding to FDCs in germinal centers with (confocal) microscopy (Supplementary methods), but this assay was discarded due to a poor signal-to-noise-ratio and complications with preparing suitable tonsil slices and tissue slice cultures. Another trial was the generation of influenza hemagglutinin immune complexes (HA-ICs) for a competition assay with PE-ICs (Supplementary methods), which showed that HA-ICs could displace PE-ICs from Raji-associated CR2s when present at an equal ratio and in excess (Supplementary Figure S4). However, this was not further explored in the current project due to time restraints.

Future experiments in this line of research include biologically relevant assays such as antigen displacement on tonsil-derived FDCs or IC-handover assays. The latter could contribute to unravelling the mechanisms of IC-handover in germinal centers using PE-ICs and the HEK-CR/U937-CR cells, since these adherent and suspension cells could be separated following PE-IC incubation and analysed using flow cytometry. In addition, the decoy receptors described in this project could be included to observe how this affects IC handover or retention. Ultimately, the assays and decoys described could be applied to study the larger-scale regulatory mechanisms of affinity maturation, GC termination and, by extent, the antibody response. To explore the therapeutic potential of decoy receptors for immune modulation, their binding and blocking properties should first be established in greater detail.

Conclusion

Altogether, three decoy receptors were designed and expressed for the purpose of antigen displacement and modulation of complement receptor binding. The sCR2.3d decoy exhibited strong binding to the opsonins C3b, C3d and C4b while the sCR1.3b and sCR1.4b decoys both showed weak binding to C3b and C4b. Additionally, the sCR2.3d decoy was capable of displacing immune complexes from cell-associated CR2, rendering it a promising tool for immune modulation.

These findings shed new light on the binding domains and ligands of CR1 and CR2, particularly the strong C3b- and C4b-binding capacity of the C3d-binding domain of CR2. These findings demonstrate the relevance of the current research for fundamental knowledge acquisition on complement receptors and complement-dependent processes such as affinity

maturation. Moreover, the therapeutic potential of these decoy receptors for immune modulation warrants further research.

Acknowledgements

All figures were made with a licensed version of BioRender.com and all flow cytometry data were analyzed using the CytoFlow software.

HEK-CR and U937-CR cells were kindly provided by Prof. Dr. Suzan Rooijakkers and her lab members at the UMC Utrecht. Purified opsonins were kindly provided by Dr. Søren Egedal Degn from Aarhus University. The adapted pcDNA™ 5/TO Mammalian Expression Vector and the Siglec Fc construct were kindly provided by Dr. Robert de Vries and his lab members.

Thanks to the department of Chemical Biology and Drug Discovery at Utrecht University, Prof. Dr. Geert-Jan Boons and Dr. Balthasar Heesters for hosting and supervising this research. Thanks to the Heesters group and de Vries lab members, especially Roosmarijn van der Woude and Ilhan Tomris, for additional support and advice on cloning and protein expression.

References

Allen, C. D., Okada, T., Tang, H. L., & Cyster, J. G. (2007b). Imaging of Germinal Center selection events during affinity maturation. *Science, 315*(5811), 528-531. doi:10.1126/science.1136736

Arulraj, T., Binder, S. C., Robert, P. A., & Meyer-Hermann, M. (2021). Germinal centre shutdown. *Frontiers in Immunology, 12*. doi:10.3389/fimmu.2021.705240

Bennett, K. M., Rooijakkers, S. H., & Gorham, R. D. (2017). Let's tie the knot: Marriage of complement and adaptive immunity in pathogen evasion, for better or worse. *Frontiers in Microbiology, 8*. doi:10.3389/fmicb.2017.00089

Buchmann, K. (2014). Evolution of innate immunity: Clues from invertebrates via fish to mammals. *Frontiers in Immunology, 5*. doi:10.3389/fimmu.2014.00459

Carrasco, Y. R., & Batista, F. D. (2007). B cells acquire particulate antigen in a macrophage-rich area at the boundary between the follicle and the subcapsular sinus of the lymph node. *Immunity, 27*(1), 160-171. doi:10.1016/j.immuni.2007.06.007

Cooper, M. D., & Alder, M. N. (2006). The evolution of Adaptive Immune Systems. *Cell, 124*(4), 815-822. doi:10.1016/j.cell.2006.02.001

Cyster, J. G. (2010). B cell follicles and antigen encounters of the third kind. *Nature Immunology, 11*(11), 989-996. doi:10.1038/ni.1946

Fearon, D. T., & Carter, R. H. (1995). The CD19/CR2/TAPA-1 complex of B lymphocytes: Linking natural to acquired immunity. *Annual Review of Immunology, 13*(1), 127-149. doi:10.1146/annurev.iy.13.040195.001015

Flajnik, M. F., & Kasahara, M. (2009). Origin and evolution of the adaptive immune system: Genetic events and selective pressures. *Nature Reviews Genetics, 11*(1), 47-59. doi:10.1038/nrg2703

Garcia, B. L., Zwarthoff, S. A., Rooijakkers, S. H., & Geisbrecht, B. V. (2016). Novel evasion mechanisms of the classical complement pathway. *The Journal of Immunology, 197*(6), 2051-2060. doi:10.4049/jimmunol.1600863

Gitlin, A. D., Shulman, Z., & Nussenzweig, M. C. (2014). Clonal selection in the Germinal Centre by regulated proliferation and hypermutation. *Nature, 509*(7502), 637-640. doi:10.1038/nature13300

Goenka, R., Matthews, A. H., Zhang, B., O'Neill, P. J., Scholz, J. L., Migone, T., . . . Cancro, M. P. (2013). Local Blys production by T follicular cells mediates retention of high affinity B cells during affinity maturation. *Journal of Experimental Medicine, 211*(1), 45-56. doi:10.1084/jem.20130505

Hannan, J. P. (2016). The structure-function relationships of complement receptor type 2 (CR2; CD21). *Current Protein & Peptide Science, 17*(5), 463-487. doi:10.2174/1389203717666151201192124

Hebell, T., Ahearn, J. M., & Fearon, D. T. (1991). Suppression of the immune response by a soluble complement receptor of B lymphocytes. *Science, 254*(5028), 102-105. doi:10.1126/science.1718035

Heesters, B., Chatterjee, P., Kim, Y., Gonzalez, S., Kuligowski, M., Kirchhausen, T., & Carroll, M. (2013). Endocytosis and recycling of immune complexes by follicular dendritic cells enhances B cell antigen binding and activation. *Immunity, 38*(6), 1164-1175. doi:10.1016/j.immuni.2013.02.023

Heesters, B. A., Myers, R. C., & Carroll, M. C. (2014). Follicular dendritic cells: Dynamic antigen libraries. *Nature Reviews Immunology, 14*(7), 495-504. doi:10.1038/nri3689

Heesters, B. A., Van der Poel, C. E., Das, A., & Carroll, M. C. (2016). Antigen presentation to B cells. *Trends in Immunology, 37*(12), 844-854. doi:10.1016/j.it.2016.10.003

Holers, V. M. (2014). Complement and its receptors: New insights into human disease. *Annual Review of Immunology, 32*(1), 433-459.

doi:10.1146/annurev-immunol-032713-120154

Kalli, K. R., Ahearn, J. M., & Fearon, D. T. (1991). Interaction of iC3b with recombinant isotypic and chimeric forms of CR2. *Journal of immunology (Baltimore, Md. : 1950)*, *147*(2), 590–594. https://pubmed.ncbi.nlm.nih.gov/1830068/

Krych-Goldberg, M., & Atkinson, J. P. (2001). Structure-function relationships of complement receptor type 1. *Immunological Reviews, 180*(1), 112-122. doi:10.1034/j.1600-065x.2001.1800110.x

Lambris, J. D., Ricklin, D., & Geisbrecht, B. V. (2008). Complement evasion by human pathogens. *Nature Reviews Microbiology, 6*(2), 132-142. doi:10.1038/nrmicro1824

Liu, D., & Niu, Z. (2009). The structure, genetic polymorphisms, expression and biological functions of complement receptor type 1 (CR1/CD35). *Immunopharmacology and Immunotoxicology, 00*(00), 090923083856073-12. doi:10.1080/08923970902845768

Liu, D., Xu, H., Shih, C., Wan, Z., Ma, X., Ma, W., . . . Qi, H. (2014). T–B-cell entanglement and ICOSL-driven feed-forward regulation of Germinal Centre reaction. *Nature, 517*(7533), 214-218. doi:10.1038/nature13803

Lowell, C. A., Klickstein, L. B., Carter, R. H., Mitchell, J. A., Fearon, D. T., & Ahearn, J. M. (1989). Mapping of the epstein-barr virus and c3dg binding sites to a common domain on complement receptor type 2. *Journal of Experimental Medicine, 170*(6), 1931-1946. doi:10.1084/jem.170.6.1931

Maul, R. W., & Gearhart, P. J. (2010). Aid and somatic hypermutation. *Advances in Immunology,* 159-191. doi:10.1016/s0065-2776(10)05006-6

McHeyzer-Williams, L. J., Milpied, P. J., Okitsu, S. L., & McHeyzer-Williams, M. G. (2015). Class-switched memory B cells remodel BCRS within secondary germinal centers. *Nature Immunology, 16*(3), 296-305. doi:10.1038/ni.3095

Merle, N. S., Church, S. E., Fremeaux-Bacchi, V., & Roumenina, L. T. (2015a). Complement system part I: Molecular mechanisms of activation and regulation. *Frontiers in Immunology, 6*. doi:10.3389/fimmu.2015.00262

Merle, N. S., Noe, R., Halbwachs-Mecarelli, L., Fremeaux-Bacchi, V., & Roumenina, L. T. (2015b). Complement system part II: Role in immunity. *Frontiers in Immunology, 6*. doi:10.3389/fimmu.2015.00257

Mesin, L., Ersching, J., & Victora, G. (2016). Germinal center B cell dynamics. *Immunity, 45*(3), 471-482. doi:10.1016/j.immuni.2016.09.001

Meyer-Hermann, M., Mohr, E., Pelletier, N., Zhang, Y., Victora, G., & Toellner, K. (2012). A theory of germinal center B cell selection, division, and exit. *Cell Reports, 2*(1),

162-174. doi:10.1016/j.celrep.2012.05.010

Phan, T. G., Grigorova, I., Okada, T., & Cyster, J. G. (2007). Subcapsular encounter and complement-dependent transport of immune complexes by lymph node B cells. *Nature Immunology, 8*(9), 992-1000. doi:10.1038/ni1494

Robbiani, D., Deroubaix, S., Feldhahn, N., Oliveira, T., Callen, E., Wang, Q., . . . Nussenzweig, M. (2015). Plasmodium infection promotes genomic instability and aid-dependent B cell lymphoma. *Cell, 162*(4), 727-737. doi:10.1016/j.cell.2015.07.019

Rodrigues, E., Jung, J., Park, H., Loo, C., Soukhtehzari, S., Kitova, E. N., Mozaneh, F., Daskhan, G., Schmidt, E. N., Aghanya, V., Sarkar, S., Streith, L., St Laurent, C. D., Nguyen, L., Julien, J. P., West, L. J., Williams, K. C., Klassen, J. S., & Macauley, M. S. (2020). A versatile soluble siglec scaffold for sensitive and quantitative detection of glycan ligands. *Nature communications, 11*(1), 5091. doi:10.1038/s41467-020-18907-6

Rooijakkers, S. H., & Van Strijp, J. A. (2007). Bacterial complement evasion. *Molecular Immunology, 44*(1-3), 23-32. doi:10.1016/j.molimm.2006.06.011

Roozendaal, R., & Carroll, M. C. (2007). Complement receptors CD21 and CD35 in humoral immunity. *Immunological Reviews, 219*(1), 157-166. doi:10.1111/j.1600-065x.2007.00556.x

Sarma, J. V., & Ward, P. A. (2010). The complement system. *Cell and Tissue Research, 343*(1), 227-235. doi:10.1007/s00441-010-1034-0

Sarrias, M. R., Franchini, S., Canziani, G., Argyropoulos, E., Moore, W. T., Sahu, A., & Lambris, J. D. (2001). Kinetic analysis of the interactions of complement receptor 2 (CR2, CD21) with its ligands C3D, ic3b, and the EBV glycoprotein GP350/220. *The Journal of Immunology, 167*(3), 1490-1499. doi:10.4049/jimmunol.167.3.1490

Schröder-Braunstein, J., & Kirschfink, M. (2019). Complement deficiencies and dysregulation: Pathophysiological consequences, modern analysis, and clinical management. *Molecular Immunology, 114*, 299-311. doi:10.1016/j.molimm.2019.08.002

Shikh, M. E., & Pitzalis, C. (2012). Follicular dendritic cells in health and disease. *Frontiers in Immunology, 3*. doi:10.3389/fimmu.2012.00292

Tiller, T., Meffre, E., Yurasov, S., Tsuiji, M., Nussenzweig, M. C., & Wardemann, H. (2008). Efficient generation of monoclonal antibodies from single human B cells by Single Cell RT-PCR and expression vector cloning. *Journal of Immunological Methods, 329*(1-2), 112-124. doi:10.1016/j.jim.2007.09.017

Toapanta, F. R., & Ross, T. M. (2006). Complement-mediated activation of the adaptive immune responses: Role of C3D in linking the innate and adaptive immunity. *Immunologic Research, 36*(1-3), 197-210. doi:10.1385/ir:36:1:197

Victora, G. D., & Nussenzweig, M. C. (2012). Germinal centers. *Annual Review of Immunology, 30*(1), 429-457. doi:10.1146/annurev-immunol-020711-075032

Victora, G. D., Schwickert, T. A., Fooksman, D. R., Kamphorst, A. O., Meyer-Hermann, M., Dustin, M. L., & Nussenzweig, M. C. (2010). Germinal center dynamics revealed by multiphoton microscopy with a photoactivatable fluorescent reporter. *Cell, 143*(4), 592-605. doi:10.1016/j.cell.2010.10.032

Victora, G. D., Dominguez-Sola, D., Holmes, A. B., Deroubaix, S., Dalla-Favera, R., & Nussenzweig, M. C. (2012). Identification of human germinal center light and dark zone cells and their relationship to human B-cell lymphomas. *Blood, 120*(11), 2240-2248. doi:10.1182/blood-2012-03-415380

Vinuesa, C. G., Sanz, I., & Cook, M. C. (2009). Dysregulation of germinal centres in autoimmune disease. *Nature Reviews Immunology, 9*(12), 845-857. doi:10.1038/nri2637

Vorup-Jensen, T., & Jensen, R. K. (2018). Structural immunology of complement receptors 3 and 4. *Frontiers in Immunology, 9*. doi:10.3389/fimmu.2018.02716

Wen, L., Atkinson, J. P., & Giclas, P. C. (2004). Clinical and laboratory evaluation of complement deficiency. *Journal of Allergy and Clinical Immunology, 113*(4), 585-593. doi:10.1016/j.jaci.2004.02.003

Wilson, J. H., & Hunt, T. (2002). Innate Immunity. In *Molecular Biology of the Cell* (4th ed.). New York: Garland Science. ISBN-10: 0-8153-3218-1

Wymann, S., Dai, Y., Nair, A. G., Cao, H., Powers, G. A., Schnell, A., . . . Hardy, M. P. (2021). A novel soluble complement receptor 1 fragment with enhanced therapeutic potential. *Journal of Biological Chemistry, 296*, 100200. doi:10.1074/jbc.ra120.016127

Zhang, Y., Meyer-Hermann, M., George, L. A., Figge, M. T., Khan, M., Goodall, M., . . . Toellner, K. (2013). Germinal center B cells govern their own fate via antibody feedback. *Journal of Experimental Medicine, 210*(3), 457-464. doi:10.1084/jem.20120150

Supplementary methods

HA-IC generation

Influenza hemagglutinin immune complexes (HA-ICs) were generated by incubating the hemagglutinin PR8 Y98F mutant (kindly provided by the de Vries group, Utrecht University)(0.4 mg/mL) with IgG CR6261 anti-HA (Creative Biolabs #TAB-735)(1 mg /mL) at a 1:4 volume ratio in GHB++ with 10% (vol/vol) serum for 30 minutes at 37℃. As negative controls, samples with heat-inactivated (HI) serum, no serum, or no hemagglutinin (HA) and anti-hemagglutinin (anti-HA) were included.

Binding assay on tonsil slices

Human tonsils (provided by the Utrecht UMC) were processed into non-fixated tissue slices and incubated with PE-ICs. Additionally, the slices were incubated with anti-C3b conjugated to FITC to detect CR-bound native ICs. The proportion of CR-bound PE-ICs to CR-bound native ICs was investigated under different conditions using confocal microscopy (Leica Microsystems).

Competition assay

PE-ICs were incubated for 30 minutes at 37℃ with Raji cells expressing CR2. HA-ICs were then added in varying ratios and cells were incubated for another 30 minutes at 37℃. PE-IC displacement from CR2 was observed using FACS based on decreased PE intensity.

ELISA

Nunc Maxisorp™ flat-bottom 96-well plates (ThermoFisher #44-2402-21) were coated overnight at 4℃ with 100 µL PE-ICs per well. The plates were washed with phosphate-buffered saline (PBS)(ThermoFisher #10010023) and blocked with PBS + 1% bovine serum albumin (BSA)(Sigma-Aldrich #9048-46-8) for one hour at RT. The plates were then incubated for 2 hours at RT with a 2-fold serial dilution of decoy receptors in blocking buffer with a maximum concentration of 40 ng/µL in 100 µL (in triplo, including no-coat and no-decoy controls). Subsequently, the plates were washed with PBS and incubated with 1:2000 StrepMAB-Classic HRP conjugate antibody (IBA-Lifesciences #2-1509-001) for one hour at RT. The wells were then washed and incubated with 100 µL of TMB Substrate Solution (ThermoFisher #N301) for 5 minutes at RT, followed by

deactivation with 100 µL of 2M H_2SO_4 and detection of decoy binding based on absorbance at 450 nm.

Blocking assay

HEK cells (HEK293T, HEK-CR1, HEK-CR2 & HEK-CR3) were seeded in a cell culture-treated flat-bottom 96-well plate (Corning™ #10412741) at 0.1 x 10^5 cells/well. The next day, cells were incubated with PE-ICs for 30 minutes at 37℃, washed and incubated with 1 µg of decoy receptor diluted in 200 µL medium for 30 minutes at 37℃. Subsequently, the cells were washed and trypsinized (20 µL/well) for 5 minutes at 37℃ followed by resuspension in FACS buffer (1xPBS, 5% (v/v) FBS, 2 mM EDTA, 2 mM NaN_3) and transfer to a round-bottom 96-well plate. The cells were then spun down for 5 minutes at 200xg and resuspended in 100 µL of 4% PFA followed by a 10 minute incubation at RT. The cells were then spun down again, resuspended in 200 µL of FACS buffer and analysed using flow cytometry. Data were collected using the BD FACSCanto II machine and analyzed using CytoFlow software. Controls with HI-serum, no serum, no ICs and no decoy receptors were included and all samples were run in triplo.

Binding assay optimization

To find the optimal ratio of PE to anti-PE, both were two-fold diluted in a 96-well plate resulting in volume ratios ranging from 256:1 to 1:556 (Supplementary Table 1) with 100,000 cells added per well. In a second experiment, PE and anti-PE were both 1.25-fold diluted resulting in volume ratios between 1:1.1 and 1:48 (Supplementary Table 2) with 10,000 cells added per well. These optimizations revealed an ideal PE:anti-PE volume ratio of 1:8, which corresponds to one molecule of PE to 128 molecules of anti-PE (**Figure 6,** Supplementary Figure 2). Moreover, the ideal IC-to-cell ratio for binding assays was established at 1 µL of PE per 100,000 Raji cells (Supplementary Figure 2).

Supplementary results

Supplementary Table S1. PE-IC optimization layout. PE to anti-PE volume ratios ranged from 256:1 to 1:1556. 100,000 Raji cells were added per well. Sample numbers are indicated in italics.

PE (µL) αPE (µL)	1	0.5	0.25	0.125	0.063	0.031	0.016	0.008	0.004	0.002	0.001	Controls
0.5	*1*	*2*	*3*	*4*	*5*	*6*	*7*	*8*	*9*	*10*	*11*	*12* - No serum
0.25	*13*	*14*	*15*	*16*	*17*	*18*	*19*	*20*	*21*	*22*	*23*	*24* - HI-serum
0.125	*25*	*26*	*27*	*28*	*29*	*30*	*31*	*32*	*33*	*34*	*35*	*36* - No PE-IC
0.0625	*37*	*38*	*39*	*40*	*41*	*42*	*43*	*44*	*45*	*46*	*47*	
0.031	*48*	*49*	*50*	*51*	*52*	*53*	*54*	*55*	*56*	*57*	*58*	
0.0156	*59*	*60*	*61*	*62*	*63*	*64*	*65*	*66*	*67*	*68*	*69*	
0.0078	*70*	*71*	*72*	*73*	*74*	*75*	*76*	*77*	*78*	*79*	*80*	
0.0039	*81*	*82*	*83*	*84*	*85*	*86*	*87*	*88*	*89*	*90*	*91*	

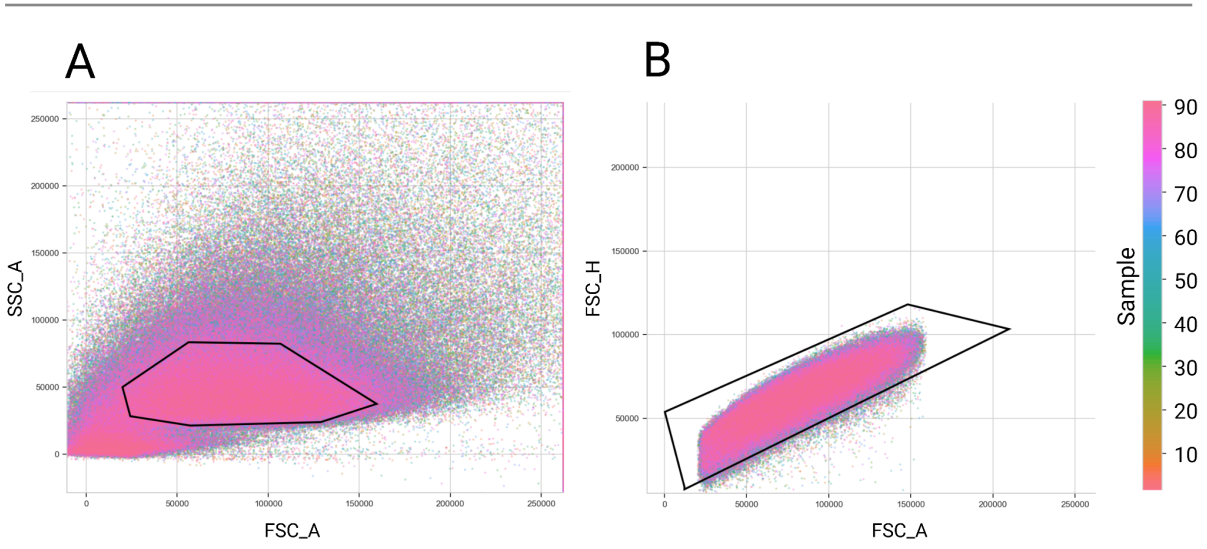

Supplementary Figure S1. Gating for binding assay optimization. A) Lymphocyte gate. B) Single cell gate.

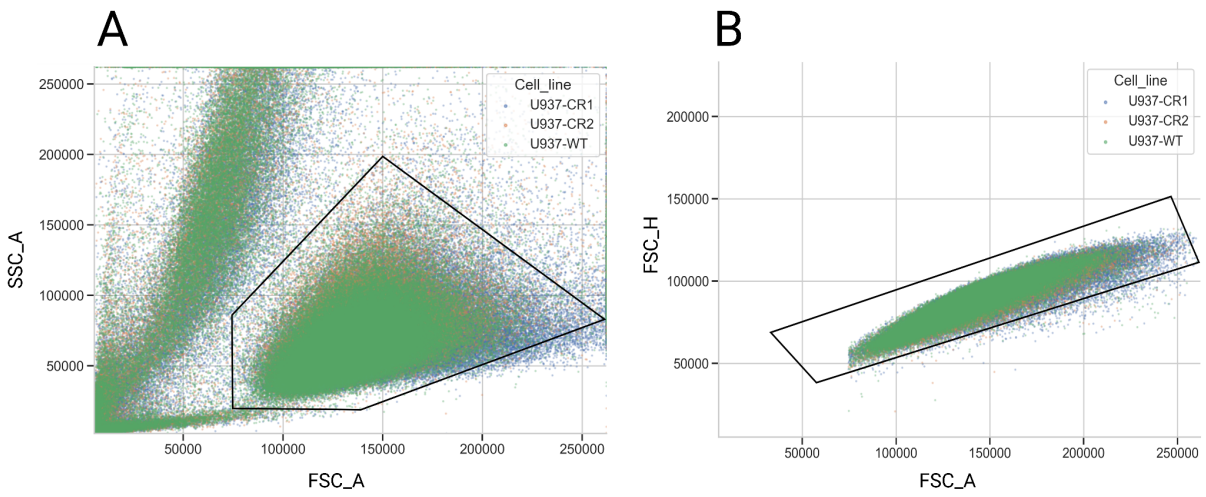

Supplementary Figure S2. Gating for U937-CR blocking assay. A) U937 cell gate. B) Single cell gate.

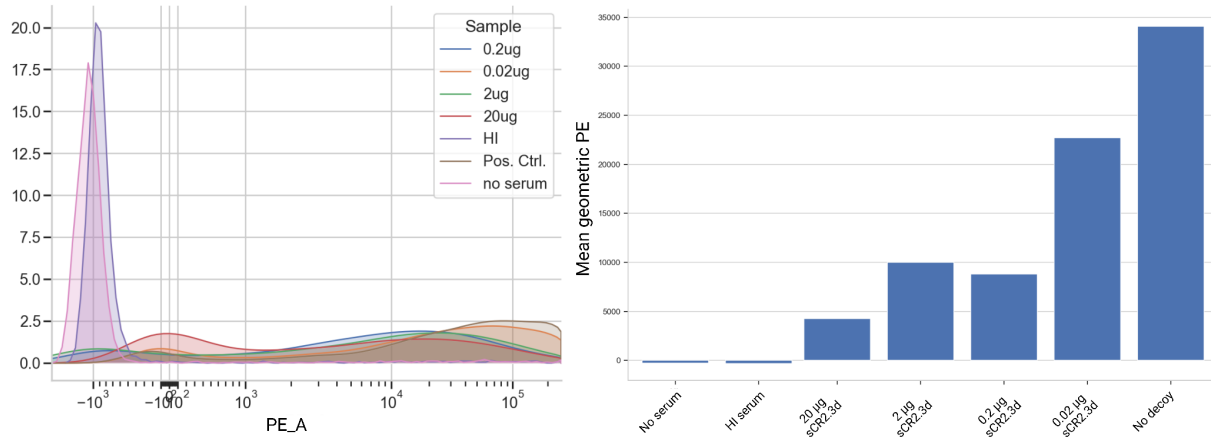

Supplementary Figure S3. Preliminary blocking experiment on Raji cells. Mean geometric PE (right panel) implies a concentration-dependent blocking of the sCR2.3d decoy on Raji cells expressing CR2. No serum and HI-serum negative controls yielded no PE signal.

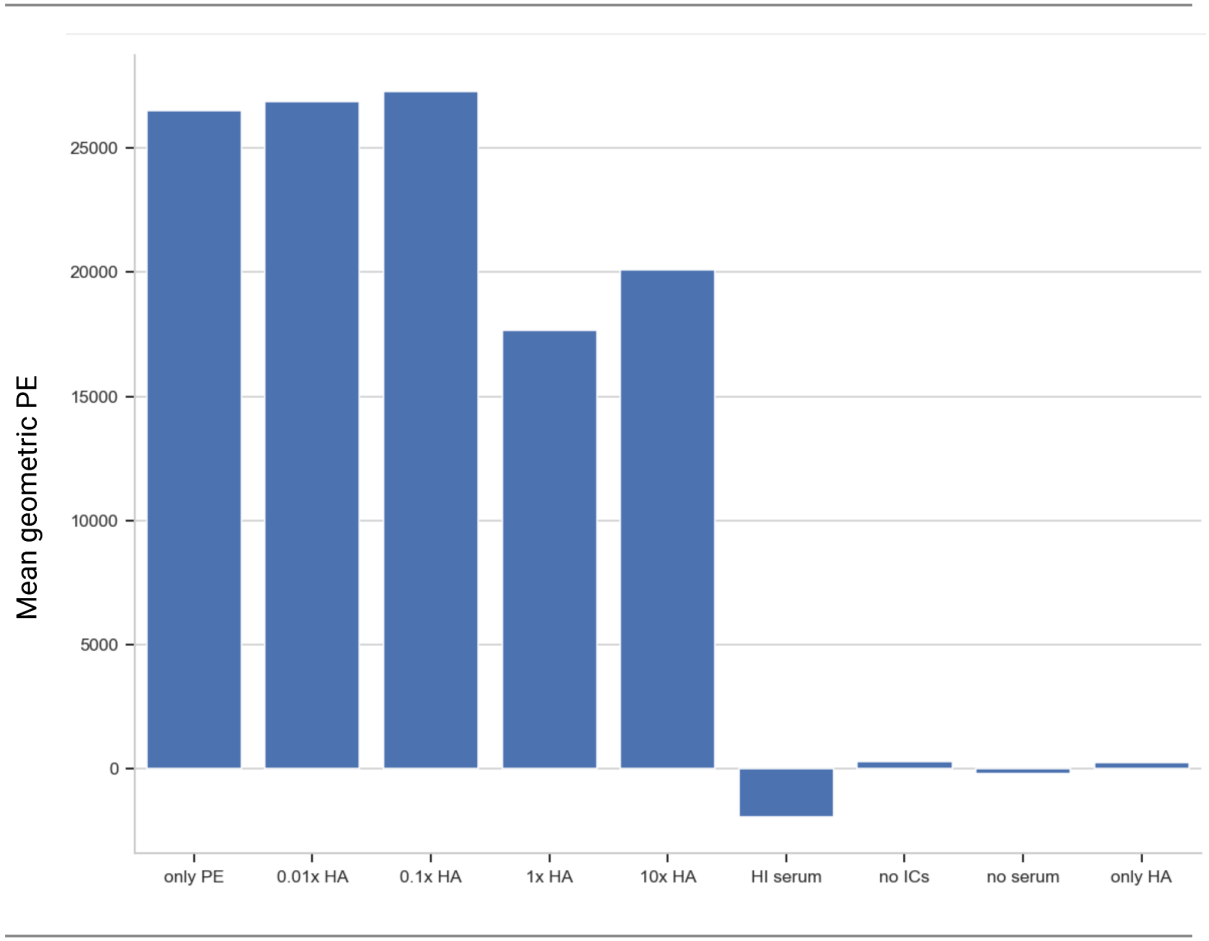

Supplementary Figure S4. Competition assay trial. Conditions indicate ratio of HA-ICs to PE-ICs added and controls. Partial displacement of PE-ICs from Raji-associated CRs was observed for the conditions with equal amounts of PE-ICS and HA-ICs and ten times as many HA-ICs as PE-ICs. Negative controls yielded no PE signal. *PE = PE-IC, HA = HA-IC.*